

1

**BETHUNE et al. Long fragment capture and sequencing**

2

**Long-fragment targeted capture for long read sequencing of  
3 plastomes**

4 Bethune Kevin<sup>1\*</sup>; Mariac Cedric<sup>1\*</sup>; Couderc Marie<sup>1</sup>; Scarcelli Nora<sup>1</sup>; Santoni Sylvain<sup>2</sup>; Ardisson Morgane<sup>2</sup>;  
5 Martin Jean-Francois<sup>3</sup>; Montufar Rommel<sup>4</sup>; Valentin Klein<sup>1</sup>; Francois Sabot<sup>1</sup>; Vigouroux Yves<sup>1</sup>; Couvreur  
6 L.P. Thomas<sup>1</sup>

7 <sup>1</sup>IRD, DIADE, Univ Montpellier, Montpellier, France

8 <sup>2</sup>UMR AGAP, Equipe Diversité et Adaptation de la Vigne et des Espèces Méditerranéennes, INRA, 2  
9 Place Viala, 34060 Montpellier, France

10 <sup>3</sup>CBGP, Montpellier SupAgro, INRA, CIRAD, IRD, Univ Montpellier, Montpellier, France

11 <sup>4</sup>Facultad de Ciencias Exactas y Naturales, Pontificia Universidad Católica del Ecuador, Quito, Ecuador

12 \* both authors contributed equally to the work

13 Manuscript received \_\_\_\_; revision accepted \_\_\_\_.

14 Number of words: 3678

15 **ABSTRACT**

16 Third generation sequencing methods generate significantly longer reads than those produced using  
17 alternative sequencing methods. This provides increased possibilities to better study biodiversity,  
18 phylogeography and population genetics. We developed a protocol for in-solution enrichment  
19 hybridization capture of long DNA fragments applicable to complete chloroplast genomes. The protocol

20 uses cost effective in-house probes developed via long-range PCR and was used in six non-model  
21 monocot species (Poaceae: African rice, pearl millet, fonio; and three palm species). DNA was extracted  
22 from fresh and silicagel dried leaves. Our protocol successfully captured long read chloroplast fragments  
23 (up to 4 264 bp median) with an enrichment rate ranging from 15% to 98%. DNA extracted from silicagel  
24 dried leaves led to low quality plastome assemblies when compared to freshly extracted DNA. Our  
25 protocol could also be generalized to capture long sequences from specific nuclear fragments.

26

27 **Keywords:** MinION, DNA probes, long-range PCR, whole chloroplast sequencing, De Novo assembly

## 28 INTRODUCTION

29 High throughput sequencing is revolutionizing research in plant evolutionary biology. The development  
30 of second generation sequencing (SGS) led to a massive amount of sequence data to be generated in a  
31 cost effective way (Straub et al. 2012). Besides the many advantages of SGS one shortcoming is that they  
32 generate short reads (between 100-400 base pairs (bp)). This is problematic for *de novo* assemblies of  
33 plant genomes that prove difficult in resolving repetitive sequences due to transposable elements,  
34 polyploidy and large genome sizes.

35 In contrast to SGS, third generation sequencing (TGS) directly targets single DNA molecules  
36 without prior PCR, enabling “real time sequencing” (Bleidorn 2016). The main improvement of TGS is the  
37 significant increase in read length from tens to tens of thousands of bases per single read (termed ‘long  
38 reads’). This provides important advantages to improve *de novo* assemblies (Jiao and Schneeberger  
39 2017), gap filling (Eckert et al. 2016) or phasing (Laver et al. 2016). Technologies such as Pacific  
40 Biosciences (PacBio) and Oxford Nanopore Technologies (ONT) are able to generate mean read lengths  
41 ranging from 5kbp to 200kbp in standard analyses (and peak up to 2 mbp) depending on the quality of

42 the DNA (Lee et al. 2016). One drawback is that most TGS technologies have high error rates when  
43 compared to SGS ( $\sim 10\%$  for ONT MinION versus 0.1% for Illumina, Goodwin et al. 2016). However, new  
44 base calling algorithms, associated with *a posteriori* corrections, allow for a significant decrease  
45 sequence errors. With sufficient coverage and proper algorithms, TGS can lead to assemblies with  
46 consensus nucleotide accuracy of 99.90% (Lee et al. 2016).

47 The application, however, of TGS using MinION to complex genomes such as plants is  
48 problematic mainly because of the generally low output of data currently available (10-20 Gb versus  
49 1,500 Gb for a HiSeq4000, Illumina). Thus, efficiently sequencing specific regions will depend on genome  
50 reduction approaches, such as targeted sequencing (Cronn et al. 2012; Jones and Good 2016). Genome  
51 reduction *via* sequence capture refers to DNA fragments (nuclear, ribosomal or plastid) that are directly  
52 captured from a total genomic library using probes binding to the complementary DNA sequences. This  
53 approach has the advantage of being cost effective, optimizes read depth on the targeted region and  
54 allows to analyze more samples per run. However, sequence capture is only routinely undertaken on  
55 short DNA fragments (Mamanova et al. 2010; Cronn et al. 2012), limiting its usefulness for long read  
56 based TGS.

57 Sequencing of complete chloroplasts or plastomes have been shown to be a marker of choice for  
58 the study plant evolution (Mariac et al. 2014; Twyford & Ness 2017). *De novo* assembly of plastomes  
59 based on short reads can be problematic (Mariac et al. 2014) leading to low quality reference plastomes.  
60 This is especially true for non-model taxa where no high quality reference genomes are available. Given  
61 the low output of data from MinION, this technology cannot be easily used to sequence plastomes  
62 directly from genomic DNA (e.g. genome skimming). The main challenge in order to efficiently apply TGS  
63 to the study of plant evolution will be based on our ability to capture long DNA fragments. To date long  
64 read targeted capture has mainly been undertaken on simple organism such as bacteria or virus (e.g.

65 Eckert et al. 2016) and rarely in complex organisms such as plants. Protocols for DNA enrichment for  
66 segments in excess of 20kbp in length have also been developed (Dapprich et al. 2016). In plants, few  
67 studies have undertaken long read targeted capture (Giolai et al. 2016, 2017). These protocols prove that  
68 capturing long fragments is possible but has yet to be routinely developed for plants.

69 Here, we present a protocol to capture long reads for plastome sequencing and reassembling  
70 using ONT MinION technology. We first developed our protocol for the model plant species *Oryza sativa*  
71 (Asian rice). We then applied the protocol to sequence plastomes in several wild species and non-model  
72 but economically important crops. Finally, we tested the ability to capture and assemble plastomes from  
73 DNA extracted silicagel dried leaves.

74

## 75 MATERIAL AND METHODS

76 *Sampling strategy and DNA extraction*

77 For this study, we focused on seven economically important plant species from Asia, Africa and South  
78 America. First, we developed and validated our long read capture protocol using the model plant species  
79 *Oryza sativa* (Asian rice). We then applied our protocol to several other plant species from the same  
80 genus (*Oryza*), family (*Poaceae*) and finally super-order (*Liliaceae* or Monocotyledons): African rice (*Oryza*  
81 *glaberrima* Steud.), a close relative to Asian rice, Pearl Millet (*Cenchrus americanus* (L.) Morrone  
82 (*Pennisetum glaucum*)), Fonio (*Digitaria exilis* Stapf.), and three species of palms: *Podococcus acaulis*  
83 Hua, *Raphia textilis* Welw. and *Phytelephas aequatorialis* Spruce (Table 1, Table S1). Export of *Podococcus*  
84 *acaulis* and *Phytelephas aequatorialis* silicagel dried leaves were authorized by the Centre national de la  
85 recherche scientifique (CENAREST, Gabon) and the Ministerio del Ambiente (Ecuador), respectively.

86 DNA was extracted from fresh leaves for *O. sativa*, *O. glaberrima*, *C. americanus* and *D. exilis*; while  
87 silicagel dried leaves were used for DNA extraction for *Podococcus acaulis*, *Raphia textilis* and  
88 *Phytelephas aequatorialis*. In both cases DNA extraction was performed using a MATAB lysis buffer and  
89 chloroform isoamyl alcohol (24:1) purification method following Mariac et al. (2006).

90 *General probe design*

91 Long fragment chloroplast sequences were captured from the total genomic DNA extracts using two  
92 different sets of biotinylated probes: one based on *O. sativa* and used on related Poaceae species (*O.*  
93 *glaberrima*, *C. americanus*, *D. exilis*) and one based on *P. barteri* Mann & H.Wendl. and used for *P.*  
94 *acaulis*, *R. textilis* and *P. aequatorialis*. Probe production (Figure 1, Supplementary file for detailed steps)  
95 was undertaken following the protocol described elsewhere (Cronn et al. 2012; Mariac et al. 2014) and  
96 lead to an average probe size of 300 bp: first, an initial full length chloroplast was amplified by long range  
97 PCR (LRPCR), using 11 primer pairs taken from Scarcelli et al. (2011) for *O. sativa* (Table S2), and another  
98 set of 11 primer pairs taken from Faye et al (2016) for *P. barteri* (Table S2). LR-PCR were carried out using  
99 the LongAmp Taq PCR kit (New England BioLabs® Inc., #E5200S) following the manufacturer's instruction  
100 in a final volume of 50 µL and using 300 ng of DNA. For each probe set LR-PCR amplicons were  
101 equimolarly pooled and sheared to reach a mean size fragment of 300 bp, then ligated to adapters so  
102 that they can be PCR amplified with biotinylated primers.

103 *Library preparation, in-solution hybridization, multiplexing and sequencing*

104 Illumina type libraries were constructed following the Rohland & Reich (2012) protocol using 6-bp  
105 barcodes and Illumina indexes with some extra steps added to allow for amplification and in-solution  
106 hybridization (Figure 1, Table S3). Briefly, each high molecular weight DNAs were sheared using G-tubes  
107 (Covaris®) to a mean target size of 10 Kb. DNA fragments below 2,000 bp were removed by a sizing step  
108 performed with 0.4X ampure beads. DNA was then end-repaired, ligated with adapters (allowing PCR

109 amplifications) and then nick filled-in before performing a pre-hybridization PCR. Optimal cycle number  
110 (ranging from 5 to 12) was defined by real-time amplification (KAPA Biosystems, KK2700). After clean-up  
111 and quantification using NanoQuant and QIAxcel, library preparations were mixed with biotin-labelled  
112 probes for hybridization of the targeted regions. DNA-probe hybridization complexes were then  
113 immobilized with 100 µg of streptavidine coated magnetic beads. This step was performed using the  
114 Dynabeads™ M-280 kilobaseBINDER™ Kit (Invitrogen, ThermoFisher Scientific, #60101), which is  
115 designed for immobilizing double stranded DNA molecules longer than 2 kbp.

116 A magnetic field was applied to the resulting solution and the supernatant containing unbounded DNA  
117 was discarded. Enriched DNA fragments were then dehybridized from the beads and amplified in a 12 to  
118 15 cycles real-time PCR in order to obtain requested quantity for the Nanopore library preparation. The  
119 final libraries were then constructed following the Nanopore library preparation detailed in the 1D  
120 Amplicon by ligation (SQK-LSK108) protocol for single samples and also in the 1D Native barcoding  
121 genomic DNA (with EXP-NBD103 and SQK-LSK108) protocol. Briefly 1µg of enriched DNA was end-  
122 repaired, extended with a dA-tailing, ligated with Nanopore barcodes and then with Nanopore tether-  
123 adapter required previous to loading and sequencing on the MinION flowcell. To benefit from  
124 multiplexing and limit costs and workload, up to four individuals were equimolarily pooled using Oxford  
125 Nanopore barcodes. Prior to each run, flowcells (FLO-MIN106 R9.4 Version) were quality-tested using  
126 the MinKNOW software version-1.2.8 to ensure the presence of at least 50% (256) of active channels.  
127 Flow cells were loaded with around 275±100 fmol of capture-amplified DNA libraries.

128 *Non-enriched MiSeq data*

129 To estimate enrichment rate, we used single sample non-enriched library datasets originating from  
130 various Illumina MiSeq sequencing runs for *O. sativa*, *O. glaberrima*, *C. americanus* and *P. aequatorialis*.  
131 For *D. exilis*, *P. aucaulis*, and the *R. textilis*, we merged 10, 2 and 16 samples, respectively, of non-

132 enriched libraries to provide adequate read counts. Forward sequencing read outputs from each MiSeq  
133 runs, namely R1 files, were first demultiplexed using demultadapt script  
134 (<https://github.com/Mailol/demultadapt>) to sort reads according to a given barcodes list. Adapters at  
135 the beginning of each read from the R2 and demultiplexed R1 files were removed using cutadapt-1.2.1  
136 software (Martin 2011) with the default parameters. Reads were then filtered on their length (size >  
137 35bp) and mean quality values (Q > 30) before being paired using compare\_fastq\_paired\_v5.pl,  
138 ([https://github.com/SouthGreenPlatform/arcad-hts/blob/master/scripts/arcad\\_hts\\_3\\_synchronized\\_paired\\_fastq.pl](https://github.com/SouthGreenPlatform/arcad-hts/blob/master/scripts/arcad_hts_3_synchronized_paired_fastq.pl)) and  
139 [/arcad\\_hts\\_2\\_Filter\\_Fastq\\_On\\_Mean\\_Quality.pl](https://github.com/SouthGreenPlatform/arcad-hts_2_Filter_Fastq_On_Mean_Quality.pl)). A last trimming step using the fastx-trimmer command  
140 from the FASTX-Toolkit ([http://hannonlab.cshl.edu/fastx\\_toolkit/](http://hannonlab.cshl.edu/fastx_toolkit/)) was undertaken onto the R2 paired  
141 files to remove the last six bases of each read to ensure removal of any possible barcode present on  
142 short reads.

144 *Bioinformatics*

145 All command lines are available in the Supplementary file.

146 Using the MinION Fast5 output format, base-calling and demultiplexing were undertaken using the  
147 Albacore program v2.5.11 (<https://github.com/Albacore/albacore>). This generated a fastq file from  
148 which reads were filtered out. The average quality score was lower than 7. For each barcode a quality  
149 control using the MinionQC R script ([https://github.com/roblanf/minion\\_qc](https://github.com/roblanf/minion_qc)) was done to check for read  
150 mean length and quality scores. Reads were then trimmed using Porechop  
151 (<https://github.com/rrwick/Porechop>) in order to remove the sequencing adapters and barcodes. The  
152 only non-default setting is that splitting reads containing middle adapters was disabled, in order to avoid  
153 issues during the polishing step using Nanopolish (see below).

154 For each library the percentage of chloroplastic reads was estimated by mapping reads to a reference  
155 chloroplast genome using the Burrows-Wheeler alignment tool (bwa mem, <https://github.com/lh3/bwa>)  
156 with “-B 1” option for non-enriched short reads data and “-x ont2d” option for long reads data (Li and  
157 Durbin 2009). We then calculated the X-fold enrichment to evaluate capture efficiency (the ratio of  
158 chloroplastic reads obtained with capture relative to chloroplastic reads obtained without capture).  
159 Coverage and depth values were calculated using Bedtools (Quinlan and Hall 2010) genomecov  
160 (<https://github.com/arq5x/bedtools2>). Mismatch percentage values between mapped reads and  
161 references were recovered using Tablet v. 1.17.08.17 (Milne et al. 2010).

162 *De novo assembly of chloroplast genomes*

163 *De novo* assembly of plastomes based on the long MinION reads, we used the Flye assembler version 2.3  
164 (Kolmogorov et al. 2018). For *O. sativa*, all available reads (17,129) were assembled. For the other  
165 species, the number of reads was too high, in excess of 3000x of the reference coverage for some  
166 datasets, which caused memory usage issues. To alleviate this, the reads were randomly split into sets of  
167 approximately equal size. Each set was then assembled individually using the raw nanopore reads mode.  
168 The “min\_overlap” parameter (i.e. the minimum overlap between reads), in Flye was adjusted on a  
169 species by species basis ranging from 3 000 pb (the default value for our genome size) to 1 000 bp,  
170 depending on the medium read length for each species. This was done in order to ensure that a  
171 sufficient amount of overlaps were detected for the assembly. The draft assemblies were then polished  
172 using Nanopolish version 0.9.1 (<https://github.com/jts/nanopolish>), using minimap2 on the “map-ont”  
173 preset for the overlapping step. Finally, the assemblies were mapped on the reference sequence of each  
174 species using the dnadiff tool of MUMmer version 4.0beta2 (Kurtz et al. 2004), which directly provides  
175 alignment coordinates and global statistics such as the mean identity percentage of alignments.

176 Besides read length, the uniformity of coverage of the reference by the reads could also have an impact  
177 on the correct assembly of plastomes. This is especially problematic for low molecular weight DNA  
178 extractions (in our case from silicagel dried leaves) which resulted in shorter read lengths on average  
179 when compared to low molecular weight DNA extractions (in our case from fresh tissue). To test for the  
180 impact of the uniformity of reference coverage on the assembly, simulated reads for *P. aequatorialis*  
181 (DNA extracted from silicagel dried leaves) were generated using NanoSim v2.1.0 (Yang et al. 2017). A  
182 model was first trained on the raw real reads and then 40'000 simulated reads were generated, ensuring  
183 they have approximately the same length distribution and error model as the real reads (see results).  
184 The simulated reads were then assembled using the same workflow as above.

185

## 186 RESULTS

187 *Plastome enrichment protocol validation on Oryza sativa*

188 After read filtering (Q>7) the median length of the 12 227 mapped plastome reads was of 4 264 bp  
189 (Table 1, Figure 2A). We recovered the whole plastome with an average coverage depth of 364X for the  
190 enriched MinION library, with a standard deviation increasing from 0.25 to 0.37 between enriched and  
191 non-enriched libraries (Figure 2A, B, Table S1). The average mismatch was 11.80% (Table S1). Finally,  
192 70.8% of the reads mapped to the reference chloroplast (Figure 2D, Table S1) representing a ~5-fold  
193 increase in chloroplast reads when compared to the non-enriched MiSeq sequenced library (13.32%  
194 mapped, Table S1). The longest plastome read recovered was 25 828 bp long (Table 1).

195 *Plastome enrichment protocol applied to non-model species*

196 DNA extraction qualities were variable depending on the source of the leaf material used. Freshly  
197 extracted DNA always produced single bands (not degraded) with fragments higher than 20 kb (Table

198 S1). Silicagel extracted DNA in contrast was of lower quality generally degraded (smear present) with  
199 fragments under 20 kb long (Table S1). For the six non-model species, sequencing of the non-enriched  
200 libraries resulted in 0.63% to 7.94% of chloroplast reads (Table S1). In contrast, enriched libraries  
201 resulted in 15.7% to 98.2% chloroplast reads, corresponding to a 12 to 161-fold increase in chloroplast  
202 DNA sequences (Figure 3, Table 1, Table S1). The mean average of fragments sequenced from freshly  
203 extracted DNA was 4 279 bp versus 2 525 bp for DNA extracted from silicagel dry leaves (Figure 4A).  
204 Sequences mapped to the reference plastomes ranged mainly from 2 kb and 8 kb, depending on the  
205 species (Figure 4A). Average coverage depth was 1,988X for enriched libraries (Figure 4B, Table S1). The  
206 longest read mapped to the plastome ranged from 10 405 bp to 25 167 bp for *R. textilis* and *C.*  
207 *americanus*, respectively (Table 1).

208 *De novo assembly of chloroplast genome*

209 When DNA was extracted from fresh leaves, the chloroplast was assembled in two contigs covering most  
210 of the reference (Table 1, Figure S1 for a visual exemple in *C. americanus*). Assembled contig lengths  
211 varied from 81 053 to 12 5727 bp long. However, the assembler never managed to achieve the full  
212 assembly and circularization of a chloroplast into a single contig. For DNA extracted from silicagel dried  
213 leaves, where reads were shorter and the coverage more heterogeneous, assembly was suboptimal  
214 (Table 1, Figure S2 for a visual exemple in *Phytelephas aequatorialis*) with more final contigs (10-17),  
215 uncovered regions and sometimes misassemblies. The longest assembled contigs were also much short  
216 than for fresh DNA (Table 2). In addition, the Inverted Repeats (IRs) were also often not differentiated.  
217 Using a simulated dataset of reads uniformly distributed across the chloroplast (Figure S3) and based on  
218 the same quality as *P. aequatorialis* significantly improved assembly (Table 2). The assembler resulted in  
219 four contigs (versus 13) covering almost 99.72% (versus 87.60%) of the reference and the longest of

220 107 633 bp (versus 21 797 bp). However, the existence of two distinct repeated regions was still not  
221 resolved.

222

## 223 CONCLUSIONS

224 Here, we show that targeted capture hybridization of long plastome DNA fragments with good  
225 coverage (362 x to 3318 x) is possible in plants (Table 1, Table S1). In addition, we show a significant  
226 enrichment of our target region (the plastome) when compared to non-enriched data (Figure 2D, 3,  
227 Table S1). The different steps of our protocol (Figure 1, Supplementary file) are not fundamentally  
228 different from previous chloroplast short read capture protocols (e.g. Mariac et al. 2014) based on in-  
229 house probe preparation, shearing, adapter ligation, hybridization and finally capture (Figure 1,  
230 Supplementary file). Thus, our approach requires minimal adaptation from previous cost and time  
231 effective protocols and should therefore be of broad interest. The main technical change focused on the  
232 beads used to capture long DNA fragments. For that we used the kilobaseBINDER™ Kit of Invitrogen  
233 which is said to capture DNA fragments longer than 2 kbp. The sizing step we performed at 0.4X using  
234 ampure removes fragments smaller than 2 kb and corresponds to the maximum allowed size with the  
235 ampure beads. However, other approaches are possible to achieve sizing with higher molecular weight  
236 and could be tested (e.g. gel extraction, Automated Size Selection System).

237 When capturing plastomes across a range of difference species, we find a difference in enrichment  
238 percentage ranging from 15.7% to 98.2% of useful reads (Table 1, Figure 4). Differences in genome  
239 versus plastome ratios between species can explain the variation of on-target mapped reads percentage  
240 compared to non-enriched libraries. In general, species with smaller genomes show higher mapped read  
241 percentages. Alternatively, the material used for DNA extractions, the cellular type and the degradation

242 state, can also explain such variations. The low enrichment observed for *P. acaulis* (Table 1, Figure 3)  
243 could potentially be linked to a large genome size, although we do not have an estimate of its genome.

244 A common coverage gap is observed among the chloroplasts of the three palm species due to a  
245 region that wasn't covered by the probes (see Faye et al. 2016). Coverage depressiveness of other  
246 regions can be explained with biases that occur during DNA shearing, PCR amplification and hybridization  
247 capture, considering a CG content effect. Probe bulk normalization from long-range PCR also has to be  
248 taken into account. However, global decrease of standard deviation of enriched libraries proved a slight  
249 increase of the whole target coverage homogeneity compared with non-enriched libraries. This means  
250 that the hybridization capture performed in our protocol didn't introduce more on-target coverage  
251 heterogeneity. Nevertheless, applying an alternative capture method such as region-specific extraction  
252 (Daprich et al. 2016) could help maintaining an overall good coverage by accessing high complex,  
253 variable, repeat-masked or unknown regions that forbid adequate probe binding.

254 Probes were designed to hybridize across the whole targeted region (Figure 1), as is generally  
255 done using short read approaches (Stull et al. 2013; Mariac et al. 2014). However, a recent study showed  
256 that probes targeting small regions are also effective to capture long reads surrounding the targeted  
257 region. Indeed, Gasc & Peyret (2017) were able to reconstruct a 21.6 kbp fragment using probes  
258 designed for a small 471 bp microbial gene target. This shows that long read capture will also be very  
259 useful for targeted sequence capture of nuclear regions.

260 We demonstrated the capacity of heterologous plastome probes to capture target DNA in other  
261 species or genera in Arecaceae and Poaceae. For example, probes designed on *P. barteri* hybridized well  
262 to other palm genera in different sub families. This underlines the good portability of probes for  
263 capturing plastomes across a broad evolutionary spectrum (Stull et al. 2013), even for long fragment  
264 capture.

265 **Limits and challenges**

266 Although we were able to successfully capture long plastid fragments using our enrichment protocol,  
267 assembling plastomes from this data remains challenging. Indeed, the best assembly resulted in 2  
268 mapped contigs, and the worst one in 17 (Table 2). Assembly of plastomes is well known to be  
269 problematic (Twyford & Ness 2017) mainly because of the presence of near identical inverted repeats  
270 (IR). Indeed, the similarity of the two IRs is too high for assemblers to decipher between IRs when  
271 resolving the assembly graph for the entry and exit point of those sequences. Thus, when the size of the  
272 sequenced reads are shorter than the IRs themselves it becomes hard to the correctly assemble of the  
273 plastome into a single contig. This is visible for example in *C. americanus* (Figure S1) where the resulting  
274 two contigs do not cross one of the IR regions leading to a failure in reaching a single contig. Of course,  
275 this problem is enhanced when dealing with overall shorter reads sequenced from low molecular weight  
276 DNA (see Figure S2 for an example). In our case, fragment length recovered of DNA extracted from  
277 silicagel dried leaves was shorter than those extracted from fresh leaves (Table 1). Moreover, we  
278 observed a decrease of the average library fragment size during preparation steps and mainly after PCR  
279 because of preferential amplification of shorter fragments, as observed by Giolai et al. (2016) and Eckert  
280 et al. (2016).

281 Optimizing read length in such a way that single reads are longer than the entire IR region should  
282 significantly help in the assembly process. In this sense, DNA shearing could be removed in order to  
283 increase the average size of the reads. Technical limitations would however be 1) the ability of  
284 streptavidin beads to immobilize fragments of tens of thousands of base pairs and 2) the long range PCR  
285 amplification step of the enriched fragments which is necessary to produce an input of several hundred  
286 ng for the construction of nanopore libraries. The latter is probably the most limiting because it is  
287 difficult to produce amplicons of several tens of Kb, and even if we achieve this, representation bias are

288 to be considered. Finally, we show, via simulations, that the uniformity of read coverage across the  
289 reference are important for assembly (Table 2). Indeed, uniformly distributed reads, even of lower  
290 quality, lead to better assemblages than poor coverage of the reference (Table 2). Therefore, uniform  
291 coverage of the reference by the captured reads plays a big role in the correct and improved assembly  
292 even for suboptimal DNA extractions.

293

#### 294 **ACKNOWLEDGEMENTS**

295 This work was publicly funded through ANR (the French National Research agency) under the  
296 “Investissement d’Avenir” programme with the reference ANR-10-LABX-001-01 Labex Agro and  
297 coordinated by Agropolis Fondation. We thank Oliver Lucas from Oxford Nanopore Technologies and  
298 Christian-Julian Villabona-Arenas for help and advice. The exportation and used of the *Phytelephas*  
299 *aequatorialis* sample was authorized by Ecuador under permit MAE-DNB-CM\_2018-0082; *Podococcus*  
300 *barteri* under permits AR0020/16; AR0036/15 (CENAREST) authorized by Gabon.

301

#### 302 **AUTHOR CONTRIBUTIONS**

303 CM, YV, TLPC conceived the idea; RM, TLPC, CM, YV provided material; CM, YV, JFM, SS, AM designed the  
304 protocol; KB, CM, MC undertook the experiments; CM, KB, FS, VK analyzed the data. KB, TLPC led the  
305 writing; all authors read and commented on the final version.

306

#### 307 **LITERATURE CITED**

308 BLEIDORN C. 2016. Third generation sequencing: technology and its potential impact on evolutionary  
309 biodiversity research. *Syst. Biodivers.* 14:1–8.

310 CRONN R., KNAUS B.J., LISTON A., MAUGHAN P.J., PARKS M., SYRING J.V., UDALL J. 2012. Targeted enrichment  
311 strategies for next-generation plant biology. *Am. J. Bot.* 99:291–311.

312 DAPPRICH J., FERRIOLA D., MACKIEWICZ K., CLARK P.M., RAPPAPORT E., D'ARCY M., SASSON A., GAI X., SCHUG J.,  
313 KAESTNER K.H., others. 2016. The next generation of target capture technologies-large DNA  
314 fragment enrichment and sequencing determines regional genomic variation of high complexity.  
315 *BMC Genomics.* 17:486.

316 ECKERT S.E., CHAN J.Z.-M., HOUNIET D., THE PATHSEEK CONSORTIUM, BREUER J., SPEIGHT G. 2016. Enrichment by  
317 hybridisation of long DNA fragments for Nanopore sequencing. *Microb. Genomics.* 2.

318 FAYE A., DEBLAUWE V., MARIAC C., RICHARD D., SONKÉ B., VIGOUROUX Y., COUVREUR T.L.P. 2016. Phylogeography  
319 of the genus *Podococcus* (Palmae/Arecaceae) in Central African rain forests: Climate stability  
320 predicts unique genetic diversity. *Mol. Phylogenet. Evol.* 105:126–138.

321 GASC C., PEYRET P. 2017. Revealing large metagenomic regions through long DNA fragment hybridization  
322 capture. *Microbiome.* 5:33.

323 GOLAI M., PAAJANEN P., VERWEIJ W., PERCIVAL-ALWYN L., BAKER D., WITEK K., JUPE F., BRYAN G., HEIN I., JONES  
324 J.D.G., CLARK M.D. 2016. Targeted capture and sequencing of gene-sized DNA molecules.  
325 *BioTechniques.* 61:315–322.

326 GOLAI M., PAAJANEN P., VERWEIJ W., WITEK K., JONES J.D.G., CLARK M.D. 2017. Comparative analysis of  
327 targeted long read sequencing approaches for characterization of a plant's immune receptor  
328 repertoire. *BMC Genomics.* 18:564.

329 GOODWIN, S., MCPHERSON, J.D., & McCOMBIE, W.R. 2016. Coming of age: ten years of next-generation  
330 sequencing technologies. *Nature Reviews Genetics*, 17, 333–351.

331 JIAO W.-B., SCHNEEBERGER K. 2017. The impact of third generation genomic technologies on plant genome  
332 assembly. *Curr. Opin. Plant Biol.* 36:64–70.

333 KARAMITROS T., MAGIORKINIS G. 2015. A novel method for the multiplexed target enrichment of MinION  
334 next generation sequencing libraries using PCR-generated baits. *Nucleic Acids Res.* 43:e152–  
335 e152.

336 KOLMOGOROV M., YUAN J., LIN Y., PEVZNER P. 2018. Assembly of Long Error-Prone Reads Using Repeat  
337 Graphs. *bioRxiv*.:247148.

338 KOREN S., WALENZ B.P., BERLIN K., MILLER J.R., BERGMAN N.H., PHILLIPPI A.M. 2017. Canu: scalable and  
339 accurate long-read assembly via adaptive k-mer weighting and repeat separation. *Genome Res.*  
340 27:722–736.

341 KURTZ S., PHILLIPPI A., DELCHER A.L., SMOOT M., SHUMWAY M., ANTONESCU C., SALZBERG S.L. 2004. Versatile and  
342 open software for comparing large genomes. *Genome Biol.* 5:R12.

343 LEE H., GURTOWSKI J., YOO S., NATTESTAD M., MARCUS S., GOODWIN S., McCOMBIE W.R., SCHATZ M. 2016. Third-  
344 generation sequencing and the future of genomics. *bioRxiv*.:048603.

345 LI H., DURBIN R. 2009. Fast and accurate short read alignment with Burrows–Wheeler transform.  
346 *Bioinformatics*. 25:1754–1760.

347 LI H., HANDSAKER B., WYSOKER A., FENNELL T., RUAN J., HOMER N., MARTH G., ABECASIS G., DURBIN R. 2009. The  
348 Sequence Alignment/Map format and SAMtools. *Bioinformatics*. 25:2078–2079.

349 MAMANOVA L., COFFEY A.J., SCOTT C.E., KOZAREWA I., TURNER E.H., KUMAR A., HOWARD E., SHENDURE J., TURNER  
350 D.J. 2010. Target-enrichment strategies for next-generation sequencing. *Nat Meth.* 7:111–118.

351 MARIAC C., SCARCELLI N., POUZADOU J., BARNAUD A., BILLOT C., FAYE A., Kougbeadjio A., MAILLOL V., MARTIN G.,  
352 SABOT F., SANTONI S., VIGOUROUX Y., COUVREUR T.L.P. 2014. Cost effective enrichment hybridization  
353 capture of chloroplast genomes at deep multiplexing levels for population genetics and  
354 phylogeography studies. *Mol. Ecol. Resour.* 14:1103–1113.

355 MILNE I., BAYER M., CARDLE L., SHAW P., STEPHEN G., WRIGHT F., MARSHALL D. 2010. Tablet—next generation  
356 sequence assembly visualization. *Bioinformatics*. 26:401–402.

357 QUINLAN A.R., HALL I.M. 2010. BEDTools: a flexible suite of utilities for comparing genomic features.  
358 *Bioinformatics*. 26:841–842.

359 ROHLAND N., REICH D. 2012. Cost-effective, high-throughput DNA sequencing libraries for multiplexed  
360 target capture. *Genome Res.* 22:939–946.

361 SCARCELLI N., BARNAUD A., EISERHARDT W., TREIER U.A., SEVENO M., D'ANFRAY A., VIGOUROUX Y., PINTAUD J.-C.  
362 2011. A Set of 100 Chloroplast DNA Primer Pairs to Study Population Genetics and Phylogeny in  
363 Monocotyledons. *PLoS ONE*. 6:e19954.

364 STRAUB S.C.K., PARKS M., WEITEMIER K., FISHBEIN M., CRONN R.C., LISTON A. 2012. Navigating the tip of the  
365 genomic iceberg: Next-generation sequencing for plant systematics. *Am. J. Bot.* 99:349–364.

366 STULL G.W., MOORE M.J., MANDALA V.S., DOUGLAS N.A., KATES H.-R., QI X., BROCKINGTON S.F., SOLTIS P.S., SOLTIS  
367 D.E., GITZENDANNER M.A. 2013. A Targeted Enrichment Strategy for Massively Parallel Sequencing  
368 of Angiosperm Plastid Genomes. *Appl. Plant Sci.* 1:1200497.

369 YANG, C., CHU, J., WARREN, R. L., & BIROL, I. 2017. NanoSim: Nanopore sequence read simulator based on  
 370 statistical characterization. *GigaScience*.

371

372

373 **Tables**

374 Table 1: MinION plastome enriched library output data. The percentage of “plastome mapped reads”  
 375 was calculated using BWA to indicated reference plastomes.

Species	DNA	probe origin	total number of reads	Median read length	longest read	% of plastid reads	longest plastome read	Median plastome read length
<i>Oryza sativa</i>	fresh	<i>O. sativa</i>	17129	4627	26128	70,8	25828	4264
<i>Oryza glaberrima</i>	fresh	<i>O. sativa</i>	81361	3695	24804	98,2	24504	3398
<i>Cenchrus americanus</i>	fresh	<i>C. americanus</i>	105760	4914	25468	97,0	25167	4623
<i>Digitaria exilis</i>	fresh	<i>C. americanus</i>	141250	3783	19378	94,4	19078	3489
<i>Podococcus acaulis</i>	silicage I	<i>P. barteri</i>	202924	2486	13103	15,7	12805	2129
<i>Raphia textilis</i>	silicage I	<i>P. barteri</i>	83833	2322	10705	87,5	10405	1997
<i>Phytelephas aequatorialis</i>	silicage I	<i>P. barteri</i>	202925	2437	15132	79,0	14832	2158

376

377

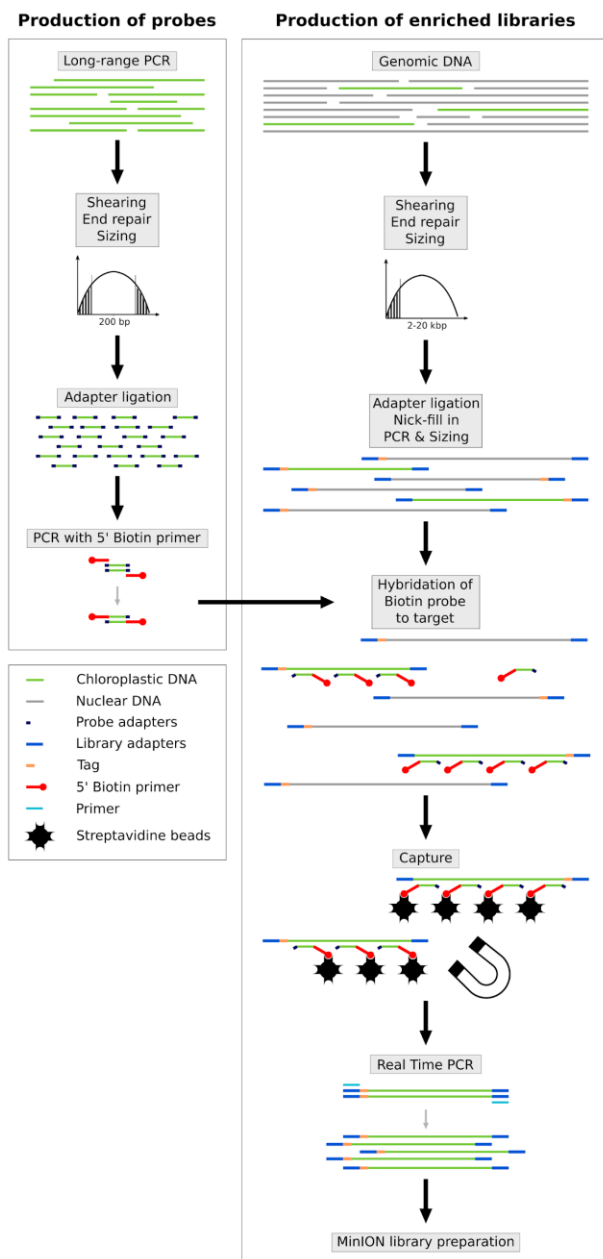
378 Table 2: De novo assembly results from real (6) and simulated (1) data in number of contigs, and  
 379 coverage and identity percentages to the respective reference plastome genomes (see Table 1). Min  
 380 overlap is the minimum overlap between reads as defined in Flye. The simulated data was based on the  
 381 out pu results of *P. aequatorialis*.

Species	Min overlap	Plastid contigs	Coverage %	Identity %	Longest contig
<i>Oryza glaberrima</i>	3000	2	92.32	99.14	109087
<i>Cenchrus americanus</i>	3000	2	99.91	98.52	81053
<i>Digitaria exilis</i>	3000	2	99.97	99.18	125727
<i>Podococcus acaulis</i>	1000	17	81.24	98.86	22803
<i>Raphia textilis</i>	1000	10	83.87	98.84	21797

<i>Phytelephas aequatorialis</i>	1000	13	87.60	98.31	20700
<i>Simulated assembly</i>	1000	4	99.72	99.05	107633

382

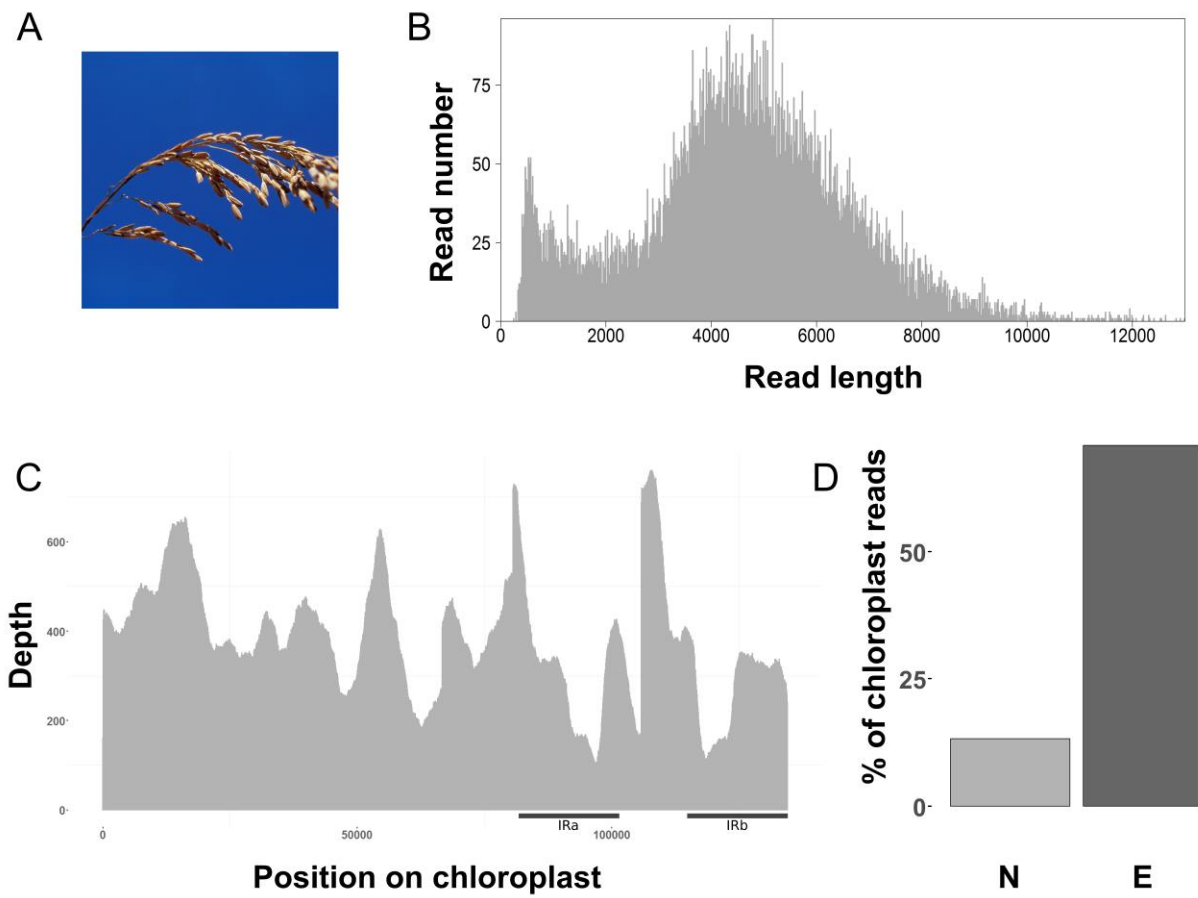
383 Figures (next page)



384

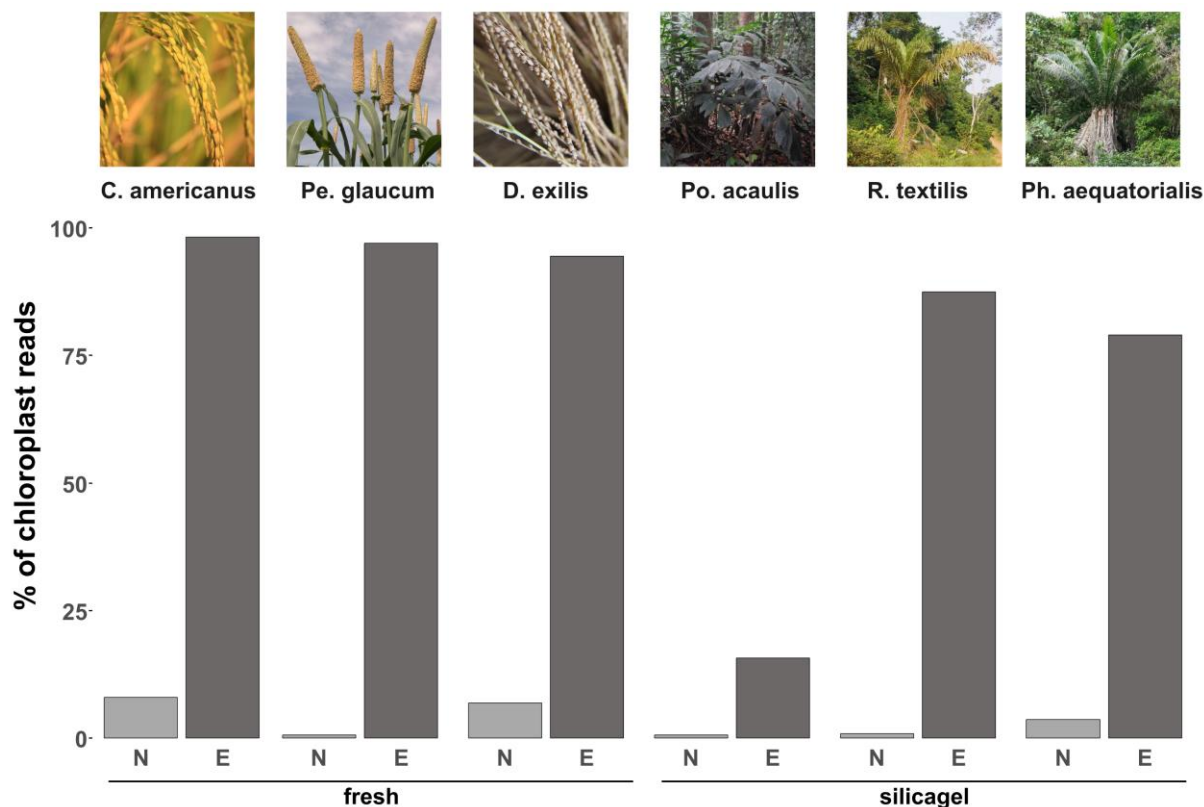
385 Figure 1: Schematic representation of the protocol used for long sequence capture of plastomes  
386 (modified from Mariac et al. 2014).

387



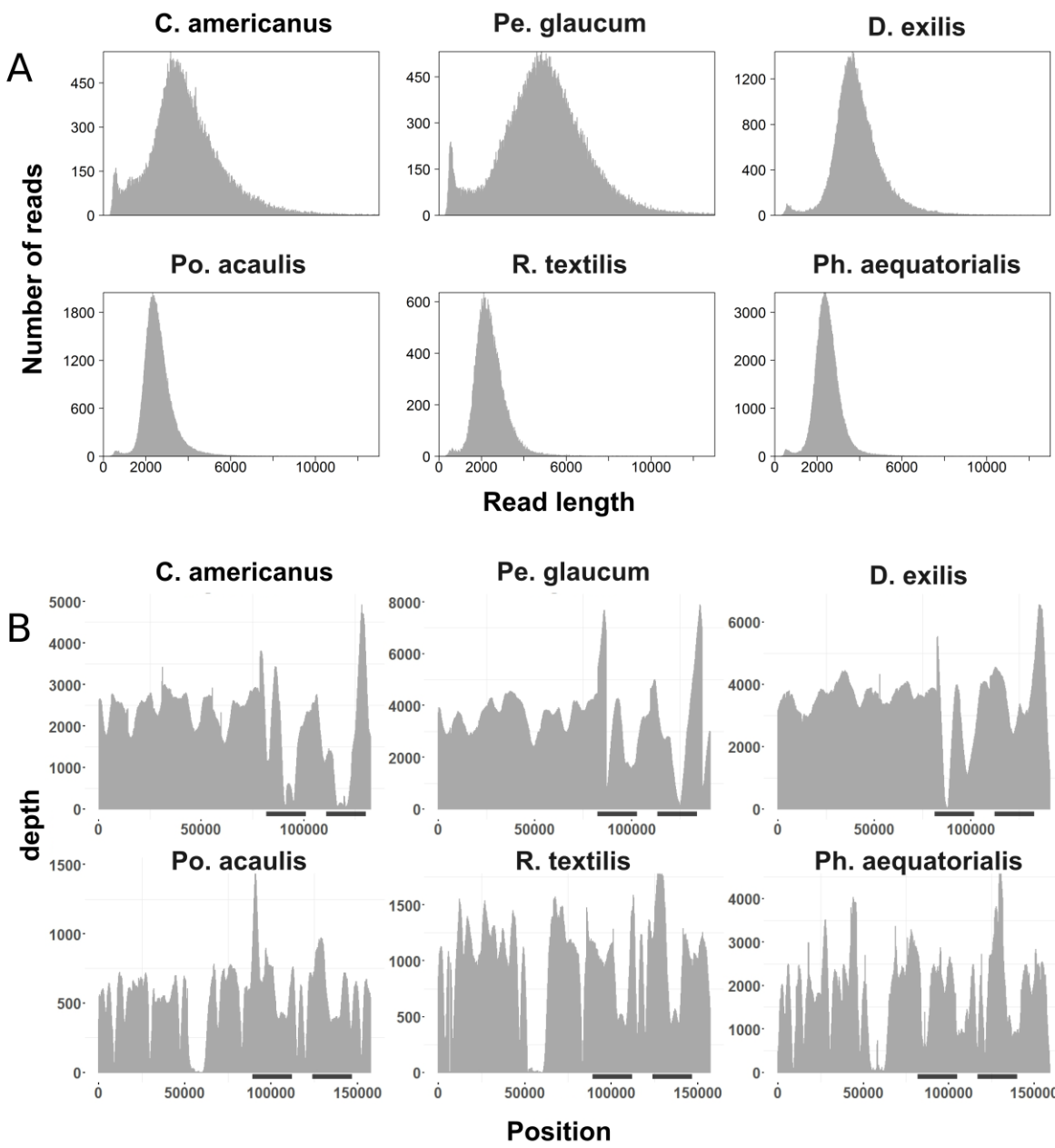
388  
389 Figure 2: Long fragment capture results for *Oryza sativa*. A: Panicle of *Oryza sativa* (Jean-Pierre  
390 Montoroi IRD ©). B: number of reads per read length before mapping. C: Plastome coverage after  
391 mapping. Black bars indicate approximate position of both inverted repeats (IR). D: Percentage of useful  
392 reads mapped to *Oryza sativa* reference plastome (KT289404.1) between non enriched (N, light grey)  
393 and enriched (E, dark grey) libraries.

394



395  
396 Figure 3: Percentage of useful reads mapped to their respective reference plastome (see Table 1)  
397 between Illumina non enriched (N, light grey) and MinION enriched (E, dark grey) protocols for the 6 non  
398 model species in our study. Photos: *O. glaberrima*: <https://pxhere.com/fr/photo/706162>; CC0 public  
399 domain; *Cenchrus americanus*: C. Mariac IRD ©; *D. exilis*: A. Barnaud IRD © ; *Po. acaulis*, *R. textilis*, *Ph.*  
400 *aequatorialis*: TLP Couvreur IRD ©.

401



402

403 Figure 4: Long fragment capture results for six non model plant species. A: Number of reads per read  
404 length before mapping. B: Plastome coverage results from the enriched long read capture protocol. Black  
405 bars indicate approximate position of both inverted repeats (IR).

406